Polymer 135 (2018) 193–199

Contents lists available at ScienceDirect

Polymer

journal homepage: www.elsevier.com/locate/polymer

Surface-initiated reversible addition-fragmentation chain transfer polymerization of chloroprene and mechanical properties of matrix-free polychloroprene nanocomposites

Yang Zheng [a, 1], Zaid M. Abbas [a, b, 1], Amrita Sarkar [a], Zachary Marsh [a], Morgan Stefik [a], Brian C. Benicewicz [a, *]

[a] Department of Chemistry and Biochemistry, University of South Carolina, Columbia, South Carolina 29208, United States
[b] Department of Chemistry, Wasit University, Hay Al-Rabea, Kut, Wasit 52001, Iraq

ARTICLE INFO

Article history:
Received 27 July 2017
Received in revised form
7 December 2017
Accepted 8 December 2017
Available online 9 December 2017

Keywords:
RAFT polymerization
Nanocomposites
Surface modification

ABSTRACT

RAFT polymerization and surface-initiated RAFT polymerization (SI-RAFT) of chloroprene was studied. The SI-RAFT polymerization rate of chloroprene was found to be slower than free solution RAFT polymerization, and further regulated by the graft density of grafted polymers. The resulting polychloroprene-grafted silica nanoparticles were directly crosslinked to obtain matrix-free polychloroprene nanocomposites that showed good nanoparticle dispersion and superior mechanical properties compared with unfilled polychloroprene rubber.

1. Introduction

Polychloroprene (PCP) has been widely used in the rubber industry since its discovery by Dupont in 1931 [1]. Compared with other elastomers, polychloroprene exhibits excellent resistance to oil, grease and wax, wide operating temperature range, and is resistant to ozone and harsh weather conditions. The application of polychloroprene ranges from adhesives and sealants, to hoses and automotive parts. To synthesize PCPs, uncontrolled free radical emulsion polymerization is commonly used with thio-based chain transfer agents to limit molecular weight [2]. The polymers synthesized in this way generally have very high molecular weight and broad molecular weight distribution. To obtain better control over the polymerization of chloroprene (CP) in recent years, controlled radical polymerization has been used to synthesize polychloroprene with predetermined molecular weight and low PDI. Topham et al. demonstrated the first controlled polymerization of chloroprene using reversible addition-fragmentation chain transfer polymerization (RAFT) [3]. Four different RAFT agents were examined in two different reaction medium (xylene and THF). The results showed that the dithioester 2-cyano-2-propylbenzodithioate exhibited the highest degree of control in xylene while 2-cyano-2-prepylbenzodithioate and a trithiocarbonate with a carboxylic acid end group were most promising in THF. Yang et al. reported on an expanded range of RAFT agents for the polymerization of chloroprene and successfully synthesized polychloroprene-block-polystyrene and poly(methyl methacrylate)-block-polychloroprene copolymers [4]. Later, Fu et al. performed reverse iodine transfer polymerization of chloroprene and studied the influence of solvent, initiator and temperature.

However, to the best of our knowledge, there are no reports on the surface initiated controlled polymerization of chloroprene to date. In fact, a broader literature search indicates that while methacrylic/acrylic and styrenic type of monomers have been grafted onto various substrates using surface initiated anionic polymerization [5], surface initiated atom transfer radical polymerization [6], surface initiated nitroxide mediated polymerization [7], and reversible fragmentation chain transfer polymerization [8], butadiene-derivative monomers such as chloroprene, have rarely been polymerized from surfaces using any of the existing controlled polymerization techniques.

It is now well accepted that the addition of nanoparticles into a

* Corresponding author.
E-mail address: benice@sc.edu (B.C. Benicewicz).
[1] These authors contributed equally.

https://doi.org/10.1016/j.polymer.2017.12.028
0032-3861/

polymer matrix can result in materials with improved thermo-mechanical properties [9]. To achieve optimal improvement, it requires that nanoparticles are well dispersed in the matrix instead of forming clusters to maximize the nanoparticle-matrix surface area. Grafting filler nanoparticles with the same polymer chains as the matrix has been demonstrated to be an effective way to improve nanoparticle dispersion. In this paper, we report the surface-initiated RAFT polymerization of chloroprene from silica nanoparticles and carefully studied polymerization kinetics at different graft densities. The resulting PCP grafted silica nanoparticles were directly crosslinked to create matrix-free nanocomposites that showed improved mechanical properties as compared to free PCP.

2. Experimental section

2.1. Materials

Chloroprene monomer was synthesized according to the literature [3]. The RAFT agent 2-methyl-2-[(dodecylsulfanylthiocarbonyl) sulfanyl]propanoic acid (MDSS) (97%) was purchased from Strem Chemicals and used as received. Spherical SiO_2 nanoparticles with a diameter of 14 ± 4 nm were purchased from Nissan Chemical Co. Tetrahydrofuran (THF) (HPLC grade, Fisher), dicumyl peroxide (Acros, 99%), and aminopropyldimethylethoxysilane (Gelest, 95%) were used as received. 2.2'-Azobisisobutyronitrile (AIBN) was purified by recrystallization from methanol and dissolved in THF to make 10 mM solutions. All other reagents were used as received.

2.2. Characterization

^{1}H NMR (Bruker ARX 300/ARX 400) was conducted using CD_3OD as the solvent. Molecular weights and dispersity were determined using a gel permeation chromatography (GPC) with a 515 HPLC pump, a 2410 refractive index detector, and three Styragel columns. The columns consist of HR1, HR3 and HR4 in the effective molecular weight ranges of 100–5000, 500–30000, and 5000–500000, respectively. THF was used as eluent at 30 °C and flow rate was adjusted to 1.0 mL/min. Molecular weights were calibrated with poly(methyl methacrylate) standards obtained from Polymer Laboratories. Dynamic Light Scattering (DLS) characterizations were conducted using Zetasizer Nano ZS90 from Malvern. Infrared spectra were obtained using a BioRad Excalibur FTS3000 spectrometer. The transmission electron microscopy (TEM) was performed on a Hitachi H8000 TEM at an accelerating voltage of 200 KV. The samples were prepared by depositing a drop of the diluted nanoparticle solution in methanol on copper grids. Scanning electron microscopy (SEM) was performed by drop-casting 10 μl of diluted nanoparticle solution on copper grids with carbon film. Small angle X-ray scattering experiments were conducted using a SAXSLab Ganesha instrument at the South Carolina SAXS Collaborative. A Xenocs GeniX3D microfocus source was used with a Cu target to generate a monochromic beam with a 0.154 nm wavelength. The instrument was calibrated using a silver behenate reference with the first order scattering vector $q^* = 1.076\ nm^{-1}$, where $q = 4\pi\lambda^{-1} \sin\theta$ with a total scattering angle of 2θ. Thermogravimetric analysis (TGA) measurements were carried out on a TA Q5000 thermogravimetric analyzer (TA Instruments). All the samples were preheated to 150 °C and kept at this temperature for 10 min to remove residual solvents. After cooling to 40 °C, the samples were heated to 800 °C with a heating rate 10 °C/min in nitrogen atmosphere. An Instron 5500 tensile tester was used to record the stress-strain curves at room temperature with a 100 N load cell and test speed of 20 mm/min. The dog-bone shaped samples for tensile testing were cut from hot pressed samples with 22 mm length and 5 mm width. Each sample was tested at least three times for tensile testing. Dynamic mechanical analysis (DMA) was measured using a RSA3 DMA (TA Instruments) in tensile mode. The DMA data was collected by testing at a frequency of 1.0 Hz, 0.1% strain and a heating rate of 3 °C/min from −100 °C to 150 °C.

2.3. Free RAFT polymerization of chloroprene

In a typical polymerization, chloroprene (0.25 g), MDSS (5.16 mg), AIBN (141μl from 10 mM stock solution) and THF (1 ml) were added and mixed well in a Schlenk flask. The mixture was degassed by three freeze-pump-thaw cycles, filled with nitrogen, and the Schlenk flask was placed in an oil bath at 60 °C. Aliquots of the reaction solution were withdrawn from the flask periodically throughout the polymerization.

2.4. Activation of 2-Methyl-2-[(dodecylsulfanylthiocarbonyl) sulfanyl]propanoic acid MDSS

MDSS (2 g, 5.49 mmol), N,N′-dicyclohexylcarbodiimide (1.24 g, 6.03 mmol) and 2-mercaptothiazole (0.718 g, 6.03 mmol) were dissolved in dichloromethane (40 mL) in a 100 mL round bottom flask under a nitrogen stream. After 10 min at room temperature, a solution of 4-dimethylaminopyridine (0.067 g, 0.549 mmol) dissolved in 2 ml of dichloromethane was added to the mixture and the nitrogen flow was removed. After 5 h at room temperature, the mixture was filtered and the solvent evaporated using a rotary evaporator. The product was subjected to column purification using a silica column with 5:4 ethyl acetate:hexane. Typical yields were 80–90%, m.p. 34–35 °C. ^{1}H NMR (300 MHz, $CDCl_3$) δ 3.20 (2H, t, S-C**H**$_2$-$(CH_2)_{10}$-CH_3), 1.97 (6H, s, C-(C**H**$_3$)$_2$), 1.71–1.15 (20H, t, S-CH_2-(C**H**$_2$)$_{10}$-CH_3), 0.89 (3H, t, SCH_2-$(CH_2)_{10}$-C**H**$_3$), 3.56 (2H, t, N-C**H**$_2$-CH_2-S), 3.92 (2H, t, S-CH_2-C**H**$_2$-N).

2.5. Synthesis of MDSS-g-SiO_2

A solution (20 mL) of colloidal silica particles (30 wt % in methyl isobutyl ketone) was added to a two-necked round bottom flask and diluted with 110 mL of THF. 3-Aminopropyldimethylethoxysilane (0.32 mL, 2 mmol) was added and the mixture was refluxed in a 65 °C oil bath for 5 h under nitrogen protection. The reaction was then cooled to room temperature and precipitated in a large amount of hexanes (500 mL). The particles were then recovered by centrifugation and dispersed in THF using sonication and precipitated in hexanes again. The amine-functionalized particles were redispersed in 40 mL of THF for further reaction. Then 0.2 g, (0.4 mmol) of activated MDSS was prepared as described above and added dropwise to a THF solution of the amine functionalized silica nanoparticles (40 mL, 6 g) at room temperature. After complete addition, the solution was stirred overnight. The reaction mixture was then precipitated into a large amount of hexanes (400 mL). The particles were recovered by centrifugation at 3000 rpm for 8 min. The particles were redispersed in 30 mL THF and precipitated in hexanes. This dissolution–precipitation procedure was repeated 2 more times until the supernatant layer after centrifugation was colorless. The yellow MDSS-anchored silica nanoparticles were dried at room temperature and analyzed using UV analysis to determine the chain density (ch/nm^2) using a calibration curve constructed from standard solutions of free MDSS. Different graft densities were achieved by adding different amounts of 3-aminopropyldimethylethoxysilane in the first step as described previously [8,10].

2.6. Surface-initiated RAFT polymerization of chloroprene

Stoichiometries of reactions were calculated using equations from our previously published literature [8,11–13]. In a typical polymerization, chloroprene (2g), MDSS-g-SiO_2 (0.74 g 0.32 ch/nm^2), AIBN (567μl from 10 mM stock solution) and THF (4 ml) were added and mixed well in a Schlenk flask. The mixture was degassed by three freeze-pump-thaw cycles, filled with nitrogen, and the Schlenk flask was placed in an oil bath at 60 °C. Aliquots of the reaction solution were withdrawn from the flask periodically throughout the polymerization. The resulting polychloroprene grafted particles were purified by two rounds of centrifugation to remove excess monomers and free polymers.

2.7. General procedure for cleaving grafted polymer from particles

In a typical experiment, 20 mg of polychloroprene grafted silica particles was dissolved in 2 mL of THF. Aqueous HF (49%, 0.2 mL) was added, and the solution was allowed to stir at room temperature overnight. The solution was poured into a PTFE Petri dish and allowed to stand in a fume hood overnight to evaporate the volatiles. The recovered polychloroprene was then subjected to GPC analyses.

2.8. Curing process of polychloroprene grafted particles

A solvent mixing technique was used for curing. All equivalents mentioned here are mass equivalents. Chloroprene polymer (100eq), zinc oxide (5eq), magnesium oxide (2eq), phenyl-α-naphthylamine (2eq), stearic acid (0.5eq), 2-mercaptothiazoline (0.5eq) were mixed well in THF (15 mL for each gram of polymer). The mixtures were then poured into Teflon petri dishes for solvent evaporation under vacuum. The dried samples were hot pressed at 160° for 25 min to obtain vulcanized rubber sheet of 0.2–0.4 mm thickness.

3. Results and discussion

2-Methyl-2-[(dodecylsulfanylthiocarbonyl) sulfanyl]propanoic acid (MDSS) was selected as the RAFT agent because it has been reported to have excellent control over a wide selection of common monomers [3], and the carboxylic acid end group provided a convenient site for grafting onto the particle surface.

We initially examined the free RAFT polymerization of CP. The ratio between species was kept at [CP]/[RAFT]/[AIBN] = 400: 1: 0.1. The reaction was carried out in THF at 60 °C, and monitored over time. As shown in Fig. 1, $\ln(M_0/M_t)$ had a linear relationship versus time and the molecular weight increased with monomer conversion although it did show a typical hybrid behavior. This hybrid behavior, resulting in an initial high molecular weight which approaches the calculated molecular weight as conversion increases, is usually ascribed to a low chain transfer constant at the initial stage of polymerization [14]. Similar behavior has also been reported for RAFT polymerization of MMA, where bimodalarity and high molecular mass at low conversion was observed as a combination of free radical polymerization and controlled radical polymerization [15]. PDI was below 1.5 during the process and the molecular weight distribution by GPC showed well-shaped unimodal peaks. We further studied the microstructure of PCP polymerized using RAFT by NMR, which has not been reported previously. It was found that the ratio between microstructures was 71% 1,4 trans, 23% cis, 1.3% 1,2 additions and 4.7% 3,4 additions. The ratio of each component is close to PCP obtained from free radical polymerization and did not change across samples of different molecular weights.

To perform surface-initiated polymerization of CP from nanoparticles, we modified particle surfaces with RAFT agents, which was realized in three steps (see Scheme 1). First, the nanoparticles were treated with an aminosilane agent to obtain amine functionalized NPs. Then MDSS was activated by reacting with 2-mercaptothiazoline followed by silica gel column for purification. Last, amine functionalized NPs were reacted with activated MDSS to obtain MDSS attached nanoparticles. Successfully functionalized NPs showed the light yellow color of MDSS, and graft density was calculated based on characteristic UV-vis absorbance of MDSS at 300 nm.

Surface-initiated RAFT polymerization of chloroprene was performed from MDSS grafted silica nanoparticles with 0.32 ch/nm^2 graft density. with ratio between [CP]/[RAFT]/[AIBN] = 400: 1: 0.1. Reaction conditions were kept exactly the same as free solution polymerization including the ratio between monomers and solvent.

The polymerization kinetics are shown in Fig. 2. Molecular weight increased with monomer conversion with slight hybrid behavior and PDIs were typically less than 1.6. The linearity of the pseudo first order kinetic plot implies a constant radical concentration during the 26 h polymerization period. These results indicated that surface anchored MDSS as well as free MDSS could be employed to control the polymerization of CP.

It is interesting to compare the reaction kinetics between free RAFT polymerization in solution, and the surface-initiated RAFT polymerization on particles. By comparing the kinetics of SI-RAFT in Fig. 2 and the one for free RAFT mediated polymerization in Fig. 1, it is obvious that the free RAFT agent mediated polymerization was much faster than SI-RAFT polymerization. Approximately 25% conversion was achieved in 4 h for free RAFT mediated polymerization and the same conversion was not achieved until 20 h for SI-RAFT with 0.32 ch/nm^2 graft density. This observation implied a retardation effect with SI-RAFT polymerization of CP. Similar observations have been reported for SI-RAFT polymerization of methyl methacrylate (MMA) using 4-cyanopentanoic acid dithiobenzoate (CPDB) as RAFT agent. We reason that such observation could be ascribed to the "localized high RAFT agent concentration" effect [8,16]. In the case of SI-RAFT polymerization, the local concentration of RAFT agent was much higher than free RAFT agent mediated polymerization due to the immobilization onto particle surfaces. Therefore, surface radicals could transfer between adjacent RAFT agents instead of propagation via monomer addition, which resulted in retardation of polymerization observed here and reported in the literature.

To provide further evidence for the hypothesis, we studied the SI-RAFT polymerization of CP with a different graft density (0.15 ch/nm^2), and plotted the reaction kinetics along with the two prior cases (Fig. 3).

We find that the kinetic curve of SI-RAFT polymerization at 0.15 ch/nm^2 graft density is intermediate between the curves of free RAFT polymerization and SI-RAFT polymerization at 0.32 ch/nm^2 density, which agrees with our hypothesis. For SI-RAFT polymerization of CP, at low-to-medium graft density, the "localized high RAFT agent concentration" effect is not as pronounced as the case for high graft density, and the polymerization kinetics was similar to the free RAFT polymerization of CP.

3.1. Mechanical properties of matrix-free PCP grafted silica nanoparticle composites

To investigate the mechanical properties of matrix-free PCP grafted silica nanoparticle composites, we prepared a series of

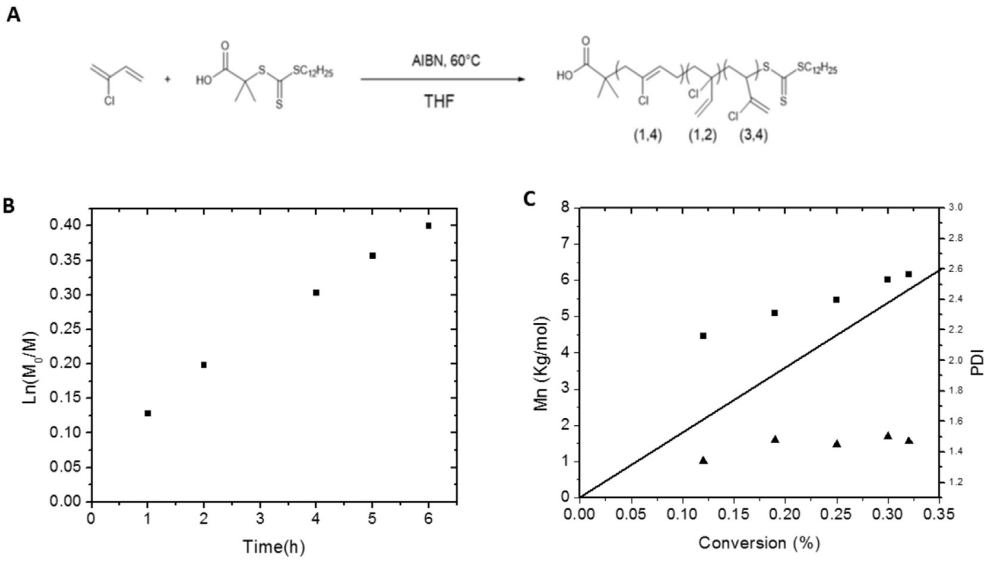

Fig. 1. (A) Reaction scheme, (B) first-order kinetic plot and (C) molecular weight and polydispersity versus conversion for RAFT polymerization of chloroprene in solution.

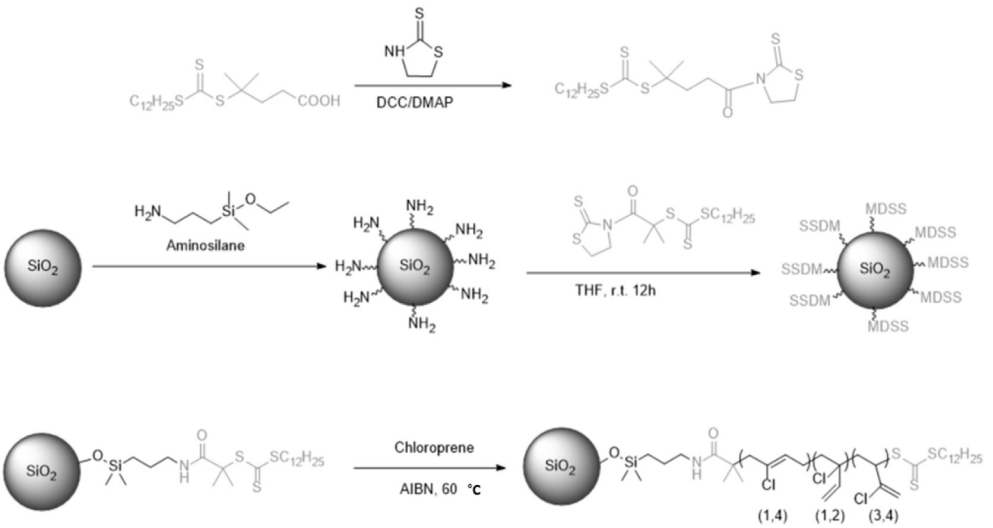

Scheme 1. Preparation of PCP grafted SiO_2 NPs.

composites from NPs with the same graft density (0.1 ch/nm^2), but different molecular weights of grafted polymer. The details of the samples are listed in Table 1.

The PCP grafted silica nanoparticles were directly crosslinked as matrix-free composites. MgO and ZnO were used as crosslinking agents. PCP grafted silica nanoparticles were mixed with curing agents in solution and then solvents were allowed to evaporate under vacuum. Dried samples were hot pressed at 160 °C for 25 min to obtain vulcanized rubber sheet of 0.2–0.4 mm thickness. The advantage of matrix-free nanocomposites over conventional composite materials is to achieve better nanoparticle dispersion. Conventional composite synthesis procedures require the mixing of particles with polymer matrix, which introduces additional complexity into the system, and often results in agglomeration of particles especially at high nanoparticle loading due to unsatisfactory interface compatibility [17]. In matrix-free systems, the particles are inherently separated from each other by the grafted polymers. Thus, good dispersion could be easily achieved [18-21].

As shown in Fig. 4, good particle dispersion was achieved with 100 kDa PCP grafted silica nanocomposites at 30 wt% silica. There was no significant clustering of particles even at high silica loading. However, a closer view revealed there is no well-defined pattern of particle distribution and interparticle spacing was not uniform, which is most likely due to the large size disparity of the core silica particles.

Small-angle X-ray scattering (SAXS) was used to obtain more information on the particle dispersion state of the crosslinked samples (see Fig. 5). No agglomeration was detected from the X-ray

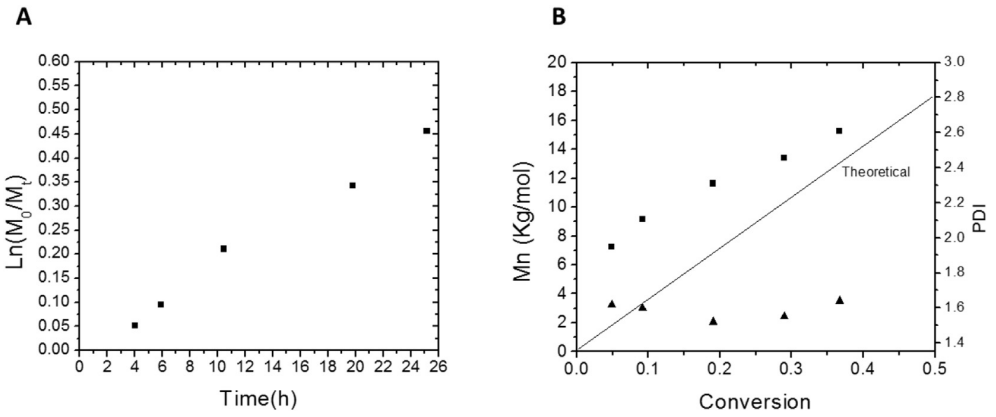

Fig. 2. (A) First-order kinetic plot and (b) molecular weight (squares) and polydispersity (triangles) versus conversion of the surfaced initiated RAFT polymerization of CP with 0.32 ch/nm^2 graft density, [CP]/[RAFT]/[AIBN] = 400: 1: 0.1.

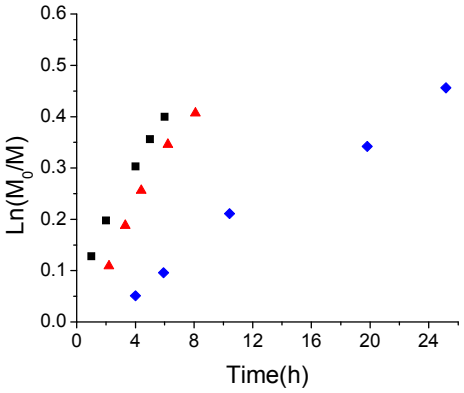

Fig. 3. Pseudo first-order kinetic plots for the polymerization of chloroprene with ratio between species [CP]/[RAFT]/[AIBN] = 400: 1: 0.1 with free MDSS (black square); MDSS grafted particles with 0.15 ch/nm^2 density (red triangle); MDSS grafted particles with 0.32 chs/nm^2 density (blue diamond). (For interpretation of the references to color in this figure legend, the reader is referred to the Web version of this article.)

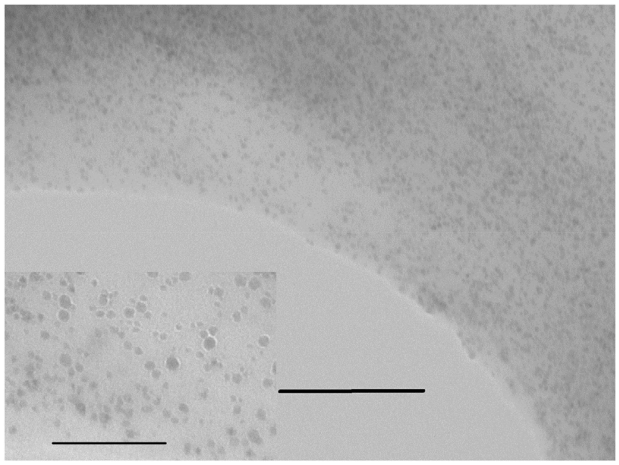

Fig. 4. TEM image of 100 kDa PCP grafted silica nanocomposites at 30 silica wt%. Scale bar 500 nm (bottom middle) and 200 nm (bottom left).

scattering pattern at low q. The intensity of all the peaks was relatively weak, indicating a broad distribution of interparticle spacing. The location of the peak did not change much between the samples, which corresponded to a d spacing ~23 nm, and seems reasonable considering the size of silica core (15 nm) plus the grafted polymers.

The matrix-free nanocomposites were crosslinked as films and cut into dog-bones for tensile testing. It was found that the properties of the composites were directly related to the silica loading of the nanocomposites.

Tensile stress-stain curves of cured matrix-free PCP silica nanocomposites are shown in Fig. 6. All the matrix-free composites had significantly improved tensile strength compared with unfilled PCP. Furthermore, the tensile stress at break increased with silica loading with a corresponding decrease in elongation at break. This general trend is consistent with previous literature that tensile strength generally increases continuously with increasing silica loading [22-24]. For matrix-free nanocomposite systems, the increase in molecular weight of the grafted polymers causes a decrease in silica loading at a fixed graft density. Thus, as

Table 1
Sample details of matrix-free PCP grafted silica nanoparticle composites.

Sample name	Graft density (ch/nm^2)	Mn (kDa)	Silica content (wt%)	Tensile strength (MPa)	Elongation at break
PCP unfilled	N/A	50	0	1.8 ± 0.11	10.3 ± 0.41
MF-47K	0.1	47	50	12.9 ± 2.19	3.9 ± 0.11
MF-55K	0.1	55	45	11.0 ± 1.21	5.3 ± 0.01
MF-70K	0.1	70	40	11.0 ± 0.76	7.7 ± 0.41
MF-100K	0.1	100	30	6.1 ± 0.59	10.9 ± 0.73

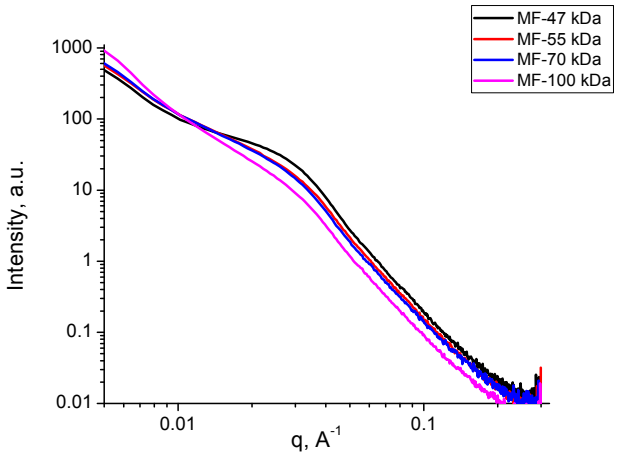

Fig. 5. Representative small-angle X-ray scattering (SAXS) intensity curves for matrix-free PCP grafted silica nanocomposites.

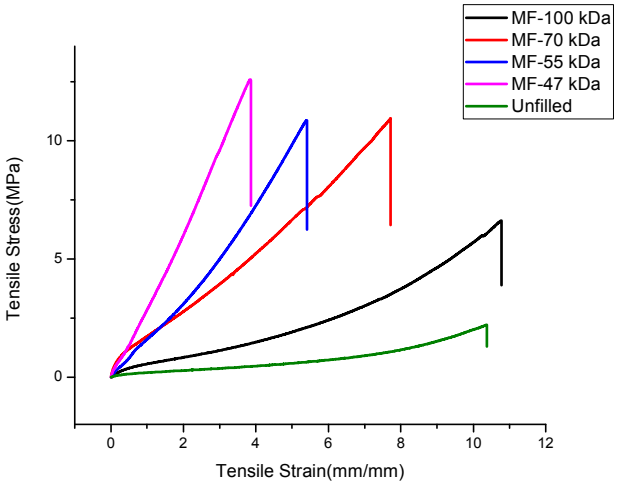

Fig. 6. Stress-strain curves of crosslinked unfilled and filled composites.

molecular weight increased, the elongation at break increased due to better entanglement between polymer chains while the tensile strength decreased due to lower silica loading. It is worth noting that the MF-100 kDa composite showed both higher tensile strength and elongation at break than unfilled polymer matrix. Typically, silica filled samples exhibit decreased tensile strain due to defects caused by particle flocculation [25], but this effect was minimized in matrix-free composites because of improved particle dispersion.

The dynamic mechanical behavior was measured at constant strain and frequency for the PCP crosslinked silica nanocomposites and the crosslinked unfilled PCP. Fig. 7A shows that at low temperatures ($T < T_g$), the effect of the silica on E' is observed even though the molecular chain segments are frozen in this region. In the rubbery plateau region, matrix-free PCP silica composites also had higher storage modulus relative to the unfilled PCP. Across matrix-free samples, the storage modulus increased with decreasing molecular weight (i.e., increasing silica content). The glass transition temperature of the matrix-free composites was not altered compared with unfilled PCP as observed in Fig. 7B, however, the reduction of tan delta peak height increased with silica loading, which also suggests better reinforcing effect and stronger rubber-filler interaction at high silica loading [26].

4. Conclusion

A facile method was demonstrated for the synthesis of polychloroprene grafted silica NPs using surface-initiated RAFT polymerization. A trithioester RAFT agent was anchored onto the surface of silica NPs with controlled graft density, and controlled radical polymerizations were conducted to produce surface grafted PCP of predetermined molecular weight and relatively narrow PDI. The polymerization kinetics was studied and it was found that the grafting-from polymerization rate was dependent on the graft density and generally slower than chloroprene polymerization mediated by free RAFT agent. The PCP grafted silica NPs were directly crosslinked to form matrix-free nanocomposites that showed uniform particle dispersion and improved mechanical properties than unfilled PCP. These strong, tough composite materials could be useful in many applications that also require the reported solvent and environmental resistance inherent in polychloroprene rubbers.

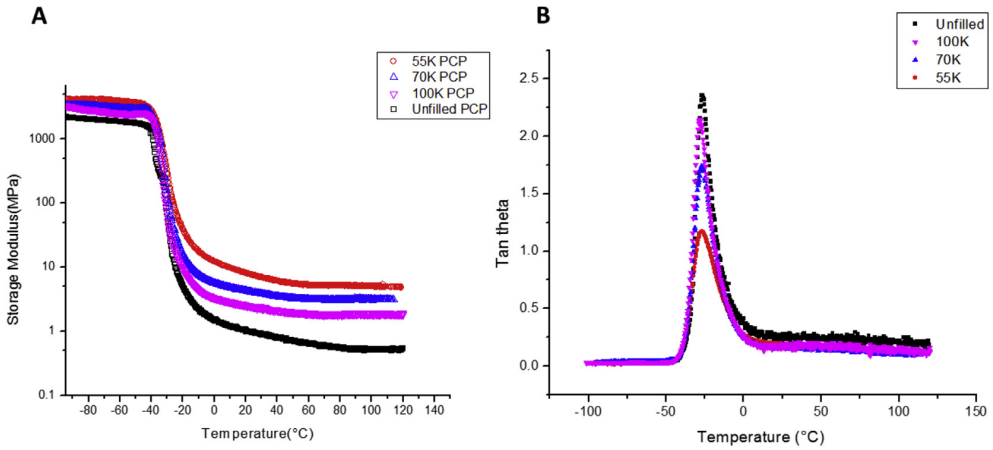

Fig. 7. Temperature dependence of storage modulus of crosslinked unfilled PCP and matrix-free PCP silica nanocomposites.

Acknowledgements

We acknowledge the support from the SC SmartState program. AS and ZM acknowledge partial support of their work as Leon Shechter graduate fellows. This work made use of the South Carolina SAXS Collaborative, supported by the NSF Major Research Instrumentation program (DMR-1428620).

References

[1] W.H. Carothers, I. Williams, A.M. Collins, J.E. Kirby, Acetylene polymers and their derivatives. II. A new synthetic rubber: chloroprene and its polymers, J. Am. Chem. Soc. 53 (11) (1931) 4203–4225.
[2] K. Itoyama, N. Hirashima, J. Hirano, T. Kadowaki, Emulsion polymerization of chloroprene. Polymerization mechanism and evaluation of crosslinking density, Polym. J. 23 (7) (1991) 859–864.
[3] N. Pullan, M. Liu, P.D. Topham, Reversible addition-fragmentation chain transfer polymerization of 2-chloro-1,3-butadiene, Polym. Chem. 4 (7) (2013) 2272–2277.
[4] J. Hui, Z. Dong, Y. Shi, Z. Fu, W. Yang, Reversible-deactivation radical polymerization of chloroprene and the synthesis of novel polychloroprene-based block copolymers by the RAFT approach, RSC Advances 4 (98) (2014) 55529–55538.
[5] Q. Zhou, X. Fan, C. Xia, J. Mays, R. Advincula, Living anionic surface initiated polymerization (SIP) of styrene from clay surfaces, Chem. Mater. 13 (8) (2001) 2465–2467.
[6] K. Ohno, T. Morinaga, K. Koh, Y. Tsujii, T. Fukuda, Synthesis of monodisperse silica particles coated with well-defined, high-density polymer brushes by surface-initiated atom transfer radical polymerization, Macromolecules 38 (6) (2005) 2137–2142.
[7] R. Matsuno, H. Otsuka, A. Takahara, Polystyrene-grafted titanium oxide nanoparticles prepared through surface-initiated nitroxide-mediated radical polymerization and their application to polymer hybrid thin films, Soft Matter 2 (5) (2006) 415–421.
[8] C. Li, J. Han, C.Y. Ryu, B.C. Benicewicz, A versatile method to prepare RAFT agent anchored substrates and the preparation of PMMA grafted nanoparticles, Macromolecules 39 (9) (2006) 3175–3183.
[9] S.K. Kumar, B.C. Benicewicz, R.A. Vaia, K.I. Winey, 50th anniversary perspective: are polymer nanocomposites practical for applications? Macromolecules 50 (3) (2017) 714–731.
[10] Y. Zheng, Y. Huang, B.C. Benicewicz, A useful method for preparing mixed brush polymer grafted nanoparticles by polymerizing block copolymers from surfaces with reversed monomer addition sequence, Macromol. Rapid Commun. 38 (19) (2017) online.
[11] Y. Zheng, L. Wang, L. Lu, Q. Wang, B.C. Benicewicz, pH and thermal dual-responsive nanoparticles for controlled drug delivery with high loading content, ACS Omega 2 (7) (2017) 3399–3405.
[12] Y. Zheng, Y. Huang, Z.M. Abbas, B.C. Benicewicz, One-pot synthesis of inorganic nanoparticle vesicles via surface-initiated polymerization-induced self-assembly, Polym. Chem. 8 (2) (2017) 370–374.
[13] Y. Zheng, Y. Huang, Z.M. Abbas, B.C. Benicewicz, Surface-initiated polymerization-induced self-assembly of bimodal polymer-grafted silica nanoparticles towards hybrid assemblies in one step, Polym. Chem. 7 (34) (2016) 5347–5350.
[14] G. Moad, C. Barner-Kowollik, The Mechanism and Kinetics of the RAFT Process: Overview, Rates, Stabilities, Side Reactions, Product Spectrum and Outstanding Challenges, Handbook of RAFT Polymerization, Wiley-VCH Verlag GmbH & Co. KGaA, 2008, pp. 51–104.
[15] C. Barner-Kowollik, J.F. Quinn, T.L.U. Nguyen, J.P.A. Heuts, T.P. Davis, Kinetic investigations of reversible addition fragmentation chain transfer Polymerizations: cumyl phenyldithioacetate mediated homopolymerizations of styrene and methyl methacrylate, Macromolecules 34 (22) (2001) 7849–7857.
[16] Y. Tsujii, M. Ejaz, K. Sato, A. Goto, T. Fukuda, Mechanism and kinetics of RAFT-mediated graft polymerization of styrene on a solid surface. 1. Experimental evidence of surface radical migration, Macromolecules 34 (26) (2001) 8872–8878.
[17] S. Prasertsri, N. Rattanasom, Fumed and precipitated silica reinforced natural rubber composites prepared from latex system: mechanical and dynamic properties, Polym. Test. 31 (5) (2012) 593–605.
[18] C.A. Grabowski, H. Koerner, J.S. Meth, A. Dang, C.M. Hui, K. Matyjaszewski, M.R. Bockstaller, M.F. Durstock, R.A. Vaia, Performance of dielectric nanocomposites: matrix-free, hairy nanoparticle assemblies and amorphous polymer–nanoparticle blends, ACS Applied Materials & Interfaces 6 (23) (2014) 21500–21509.
[19] J. Yan, T. Kristufek, M. Schmitt, Z. Wang, G. Xie, A. Dang, C.M. Hui, J. Pietrasik, M.R. Bockstaller, K. Matyjaszewski, Matrix-free particle brush system with bimodal molecular weight distribution prepared by SI-ATRP, Macromolecules 48 (22) (2015) 8208–8218.
[20] Y. Li, L. Wang, B. Natarajan, P. Tao, B.C. Benicewicz, C. Ullal, L.S. Schadler, Bimodal "matrix-free" polymer nanocomposites, RSC Advances 5 (19) (2015) 14788–14795.
[21] Y. Huang, Y. Zheng, A. Sarkar, Y. Xu, M. Stefik, B.C. Benicewicz, Matrix-free polymer nanocomposite thermoplastic elastomers, Macromolecules 50 (12) (2017) 4742–4753.
[22] P. Sae-oui, C. Sirisinha, U. Thepsuwan, K. Hatthapanit, Dependence of mechanical and aging properties of chloroprene rubber on silica and ethylene thiourea loadings, Eur. Polym. J. 43 (1) (2007) 185–193.
[23] P. Sae-oui, C. Sirisinha, U. Thepsuwan, K. Hatthapanit, Roles of silane coupling agents on properties of silica-filled polychloroprene, Eur. Polym. J. 42 (3) (2006) 479–486.
[24] B.P. Kapgate, C. Das, A. Das, D. Basu, S. Wiessner, U. Reuter, G. Heinrich, Reinforced chloroprene rubber by in situ generated silica particles: evidence of bound rubber on the silica surface, J. Appl. Polym. Sci. 133 (30) (2016) (n/a-n/a).
[25] L. Qu, L. Wang, X. Xie, G. Yu, S. Bu, Contribution of silica-rubber interactions on the viscoelastic behaviors of modified solution polymerized styrene butadiene rubbers (M-S-SBRs) filled with silica, RSC Advances 4 (109) (2014) 64354–64363.
[26] C. Kumnuantip, N. Sombatsompop, Dynamic mechanical properties and swelling behaviour of NR/reclaimed rubber blends, Mater. Lett. 57 (21) (2003) 3167–3174.